Original Article | Neuroimaging and Head and Neck

http://dx.doi.org/10.3348/kjr.2013.14.3.477
pISSN 1229-6929 · eISSN 2005-8330
Korean J Radiol 2013;14(3):477-486

Korean Journal of Radiology
KJR

Application of ^{31}P MR Spectroscopy to the Brain Tumors

Dong-Ho Ha, MD[1], Sunseob Choi, MD[1], Jong Young Oh, MD[1], Seong Kuk Yoon, MD[1], Myong Jin Kang, MD[1], Ki-Uk Kim, MD[2]

Departments of [1]Radiology and [2]Neurosurgery, College of Medicine, Dong-A University, Busan 602-715, Korea

Objective: To evaluate the clinical feasibility and obtain useful parameters of ^{31}P magnetic resonance spectroscopy (MRS) study for making the differential diagnosis of brain tumors.

Materials and Methods: Twenty-eight patients with brain tumorous lesions (22 cases of brain tumor and 6 cases of abscess) and 11 normal volunteers were included. The patients were classified into the astrocytoma group, lymphoma group, metastasis group and the abscess group. We obtained the intracellular pH and the metabolite ratios of phosphomonoesters/phosophodiesters (PME/PDE), PME/inorganic phosphate (Pi), PDE/Pi, PME/adenosine triphosphate (ATP), PDE/ATP, PME/phosphocreatine (PCr), PDE/PCr, PCr/ATP, PCr/Pi, and ATP/Pi, and evaluated the statistical significances.

Results: The brain tumors had a tendency of alkalization (pH = 7.28 ± 0.27, p = 0.090), especially the pH of the lymphoma was significantly increased (pH = 7.45 ± 0.32, p = 0.013). The brain tumor group showed increased PME/PDE ratio compared with that in the normal control group (p = 0.012). The ratios of PME/PDE, PDE/Pi, PME/PCr and PDE/PCr showed statistically significant differences between each brain lesion groups (p < 0.05). The astrocytoma showed an increased PME/PDE and PME/PCr ratio. The ratios of PDE/Pi, PME/PCr, and PDE/PCr in lymphoma group were lower than those in the control group and astrocytoma group. The metastasis group showed an increased PME/PDE ratio, compared with that in the normal control group.

Conclusion: We have obtained the clinically applicable ^{31}P MRS, and the pH, PME/PDE, PDE/Pi, PME/PCr, and PDE/PCr ratios are helpful for differentiating among the different types of brain tumors.

Index terms: *Magnetic resonance imaging; MRS; Brain; Tumor*

INTRODUCTION

Magnetic resonance spectroscopy (MRS) has been used to identify the characteristics of cancer cells and to evaluate the response of cancer cells to the targeted treatment, noninvasively, by MR signal (1). The commonly utilized elements for MRS are ^{1}H, ^{31}P, ^{13}C, ^{19}F, ^{23}NA and ^{2}H (2). The phosphorous metabolites detected by ^{31}P MRS, such as adenosine triphosphate (ATP), phosphocreatine (PCr), inorganic phosphate (Pi), phosphomonoesters (PME), and phosophodiesters (PDE), provide the information of the intracellular pH, the cellular energy metabolism, and the phospholipid metabolism (3, 4).

In brain tumors, ^{31}P MRS showed variable changes of the phospholipid metabolism. The intracellular pH and some phosphorous metabolite ratios, such as PME/PDE, PME/Pi, PDE/Pi, PME/ATP, PDE/ATP, PME/PCr and etc, were considered to be potential markers of tumors (3, 5-8).

Received May 31, 2012; accepted after revision September 4, 2012.
This study was supported by research funds from Dong-A University.
Corresponding author: Sunseob Choi, MD, Department of Radiology, College of Medicine, Dong-A University, 26 Daesingongwon-ro, Seo-gu, Busan 602-715, Korea.
• Tel: (8251) 240-5344 • Fax: (8251) 253-4931
• E-mail: sschoi317@yahoo.co.kr

However, there are several limitations. There have been reports that ^{31}P MRS has a limited role for diagnosing cancer, making the differential diagnosis of specific tumor types and assessing the degree of malignancy (3, 6, 8). Moreover, even though ^{31}P MRS showed good reproducibility among different institutions (9), many of the results did not match well with other results. The most useful metabolite ratios have not yet been agreed on. Furthermore, long scan time and the complexity of the post-processing procedure make other limitations to apply ^{31}P MRS to patients.

We performed a localized ^{31}P MRS study on brain tumorous lesions with a relatively short scan time and evaluate the useful parameters of ^{31}P MRS study to differentiate the brain tumors.

MATERIALS AND METHODS

Patients

From October 2006 to May 2010, we prospectively performed MRS study on 47 patients who had brain tumorous lesions detected on MRI. Forty five cases of brain tumor and abscess were confirmed by biopsy or open surgery.

We excluded the brain lesion that had large hemorrhage on the T1 weighted MR images. We also excluded the other brain lesions for the following reasons by a consensus of two radiologists: 1) the size of brain lesions on MRI was too small to evaluate the MRS spectrum, lesser than 3 cm in diameter, 2) two post-radiation states, 3) local recurrence after chemotherapy or radiation therapy, 4) rare cases such as pineal meningioma and dural hemangioblastoma, 5) one case of pilocytic astrocytoma that had a large cyst, was excluded from the cases of astocytoma, and 6) one case of purely cystic abscess that contained entirely cystic portion on the fluid-attenuated inversion recovery images.

As a result, we included 22 cases of brain tumor and 6 cases of abscess. The pathologically confirmed brain tumor and abscess were classified into the 13 cases of astrocytoma (age range: 16-74, mean age: 42.8, 7 males and 4 females, 4 cases of low grade astrocytoma and 9 cases of high grade astrocytoma), 4 cases of lymphoma (age range: 56-69, mean age: 64.0, 3 males and 1 female), 5 cases of metastasis (age range: 60-80, mean age: 71.8, 1 male and 4 females) and 6 cases of abscess (age range: 30-73, mean age: 54.5, 3 males and 3 females) (Fig. 1). All 4 cases of lymphoma were large B cell lymphoma. None of these patients received therapy before the MRS analysis.

We also obtained the MRS spectra of 11 normal volunteers as the control group (age range: 23-40 years, mean age: 30.2, 7 males and 4 females). They did not have any specific medical history, such as migraine, recent infarct or trauma. The MRS of normal volunteers was obtained at the thalamus area to avoid the artifact from subcutaneous fat and magnetic inhomogeneity due to a peripheral location.

MRS Protocol

We performed ^{31}P MRS on a 1.5 T GE scanner (Signa; GE Medial System, Milwaukee, WI, USA) with a flexible ^{31}P transmit/receive coil, operating at 25.85 MHz. This coil contained a blocking circuit to prevent the reception of signals at the hydrogen frequency (63.86 MHz). The patient's head was wrapped with the flexible surface phosphorus coil and placed in the hydrogen head coil for

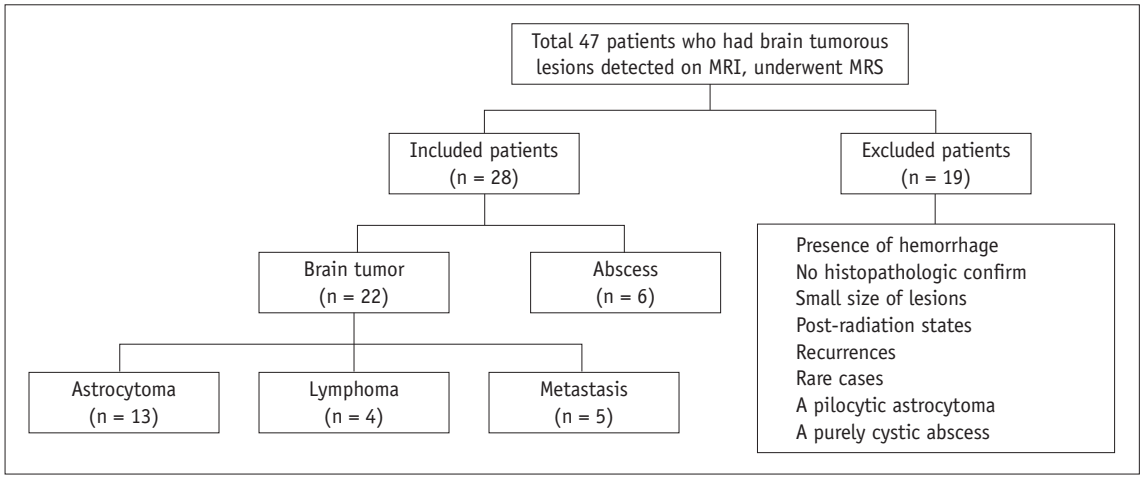

Fig. 1. Flow chart of patient selection. On basis of histopathologic results, patients were classified into 22 cases of brain tumor and 6 cases of abscess. Brain tumors were subdivided into 13 cases of astrocytoma group, 4 cases of lymphoma group, and 5 cases of metastasis group. MRS = magnetic resonance spectroscopy

Korean Journal of Radiology
KJR

localization.

For localization of a region of interest (ROI), the T2 weighted fast spin-echo sequences in two different slice orientations were performed. Then, automated ^{1}H shimming was done to obtain the homogeneity of the ROI by using the point resolved spectroscopy sequence pulse sequence.

For ^{31}P spectroscopy, the free induction decay (FID) 2 dimensional (2D) chemical shift imaging (CSI) sequence was carried out in an axial plane. The field of view was 3 x 3 x 3 cm, and the volume was 27 mL. The following parameters were used, Nex: 8, scan number: 128, spectral width: 2500 Hz, and acquired data points: 2048.

The ^{31}P spectra were post-processed using an automated procedure developed in SAGE (GE Medical Systems, Fremont, CA, USA). The obtained FID signal was displayed as a spectrum, following 2D CSI reconstruction with a magnitude channel. After using the 6 Hz exponential line broadening, we obtained the MR spectra that were assigned on the basis of prior assignment, such as PME, Pi, PDE, PCr and ATP. The chemical shift in the ^{31}P MRS referred to the position of PCr (δ = 0.00 ppm). The intracelluar pH of the lesions was calculated by using the chemical shift of Pi relative to PCr, with the formula taken from Ng et al. (10) (Fig. 2). The integral of each of the phosphorous metabolites, such as ATP, PCr, Pi, PME and PDE, was measured. The following metabolite ratios of PME/PDE, PME/Pi, PDE/Pi, PME/ATP, PDE/ATP, PME/PCr, PDE/PCr, PCr/ATP, PCr/Pi and ATP/Pi were calculated from the measured values (Figs. 3-5).

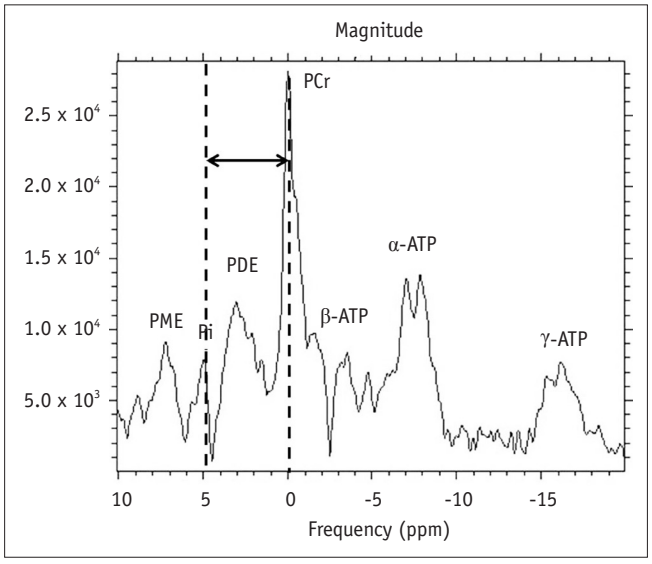

Fig. 2. Measuring pH in lesion. Intracelluar pH of brain lesions is calculated by using measured δ Pi (arrow), which is chemical shift, from PCr to Pi. PME = phosphomonoester, PDE = phosphodiester, PCr = phosphocreatine, ATP = adenosine triphosphate, Pi = inorganic phosphate

Statistical Analysis

We compared the mean values of the intracellular pH and the metabolite ratios between the normal control group and the brain tumor group by using the Mann-Whitney U test.

The Kruskal-Wallis test was used for obtaining the statistical significant parameter between the each brain lesion. Additionally, multiple comparisons of each brain lesions were also carried out using the Dunn test.

For comparison between the low grade astrocytoma group and high grade astocytoma group, and between the brain tumor group and the abscess group, the mean values of the intracellular pH and the metabolite ratios were also compared by using the Mann-Whitney U test.

A *p* value of less than 0.05 was considered significant. The statistical analysis was performed by using Statistical Package for the Social Sciences software (version 19.0, Chicago, IL, USA).

RESULTS

The average scan time for ^{31}P MRS was 6 minutes 36 seconds. Total scan time was 15 minutes, including the scanning for localization. All patients were tolerable to obtain the MR imaging and the MR spectrum in a study. The pattern of the spectrum or chemical shift frequency of each metabolite was very similar in each group.

The intracellular pH in the normal control group was calculated as 7.07 ± 0.10 (Table 1). These values were slightly higher than those of the previous reported values in a healthy volunteer group (11, 12). The brain tumors had a tendency of alkalization at a pH = 7.28 ± 0.27 (*p* value, 0.090) (Table 1). The PME/PDE ratio in the brain tumor group (0.57 ± 0.11) showed a significant increase compared to that in the control group (0.47 ± 0.07) (*p* value, 0.012).

The intracellular pH between each brain lesion groups did not show a statistically significant difference by using the Kruskal-Wallis test (Table 2). We also obtained statistical significance of the intracellular pH between the normal control group and each brain lesions by using the Mann-Whitney U test. The lymphoma had a mean pH of 7.45 ± 0.32 and this represents significant alkalization, compared to the normal control group (*p* value, 0.013). The mean value of pH in the metastasis (7.48 ± 0.56) was markedly higher than in the normal brain, but the difference was statistically insignificant (*p* value, 0.112). The pH in the

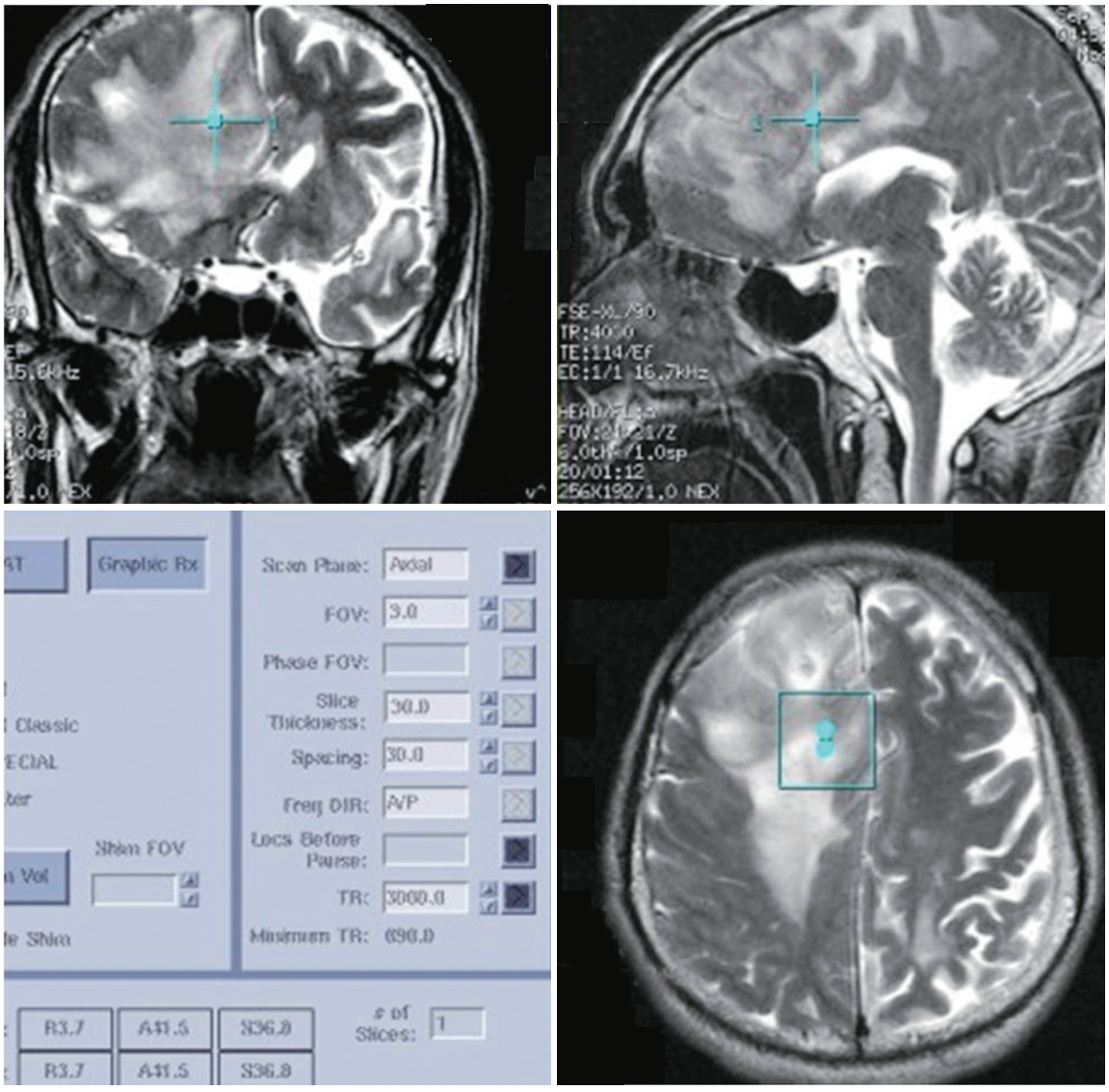

A

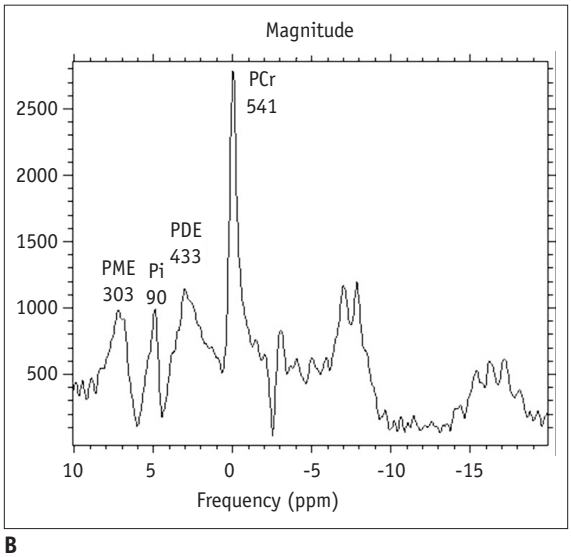

B

Fig. 3. 44-year-old man with high grade astrocytoma of brain.
A. Localizer image for ^{31}P MRS shows huge mass in right frontal lobe without cyst or hemorrhage. **B.** ^{31}P MRS shows high level of PME (303), low level of Pi (90) and relatively low level of PDE (433). Calculated PME/PDE ratio (0.70) is higher than its mean value in control group (0.47). PME = phosphomonoester, PDE = phosphodiester, PCr = phosphocreatine, MRS = magnetic resonance spectroscopy, Pi = inorganic phosphate

Korean Journal of Radiology
KJR

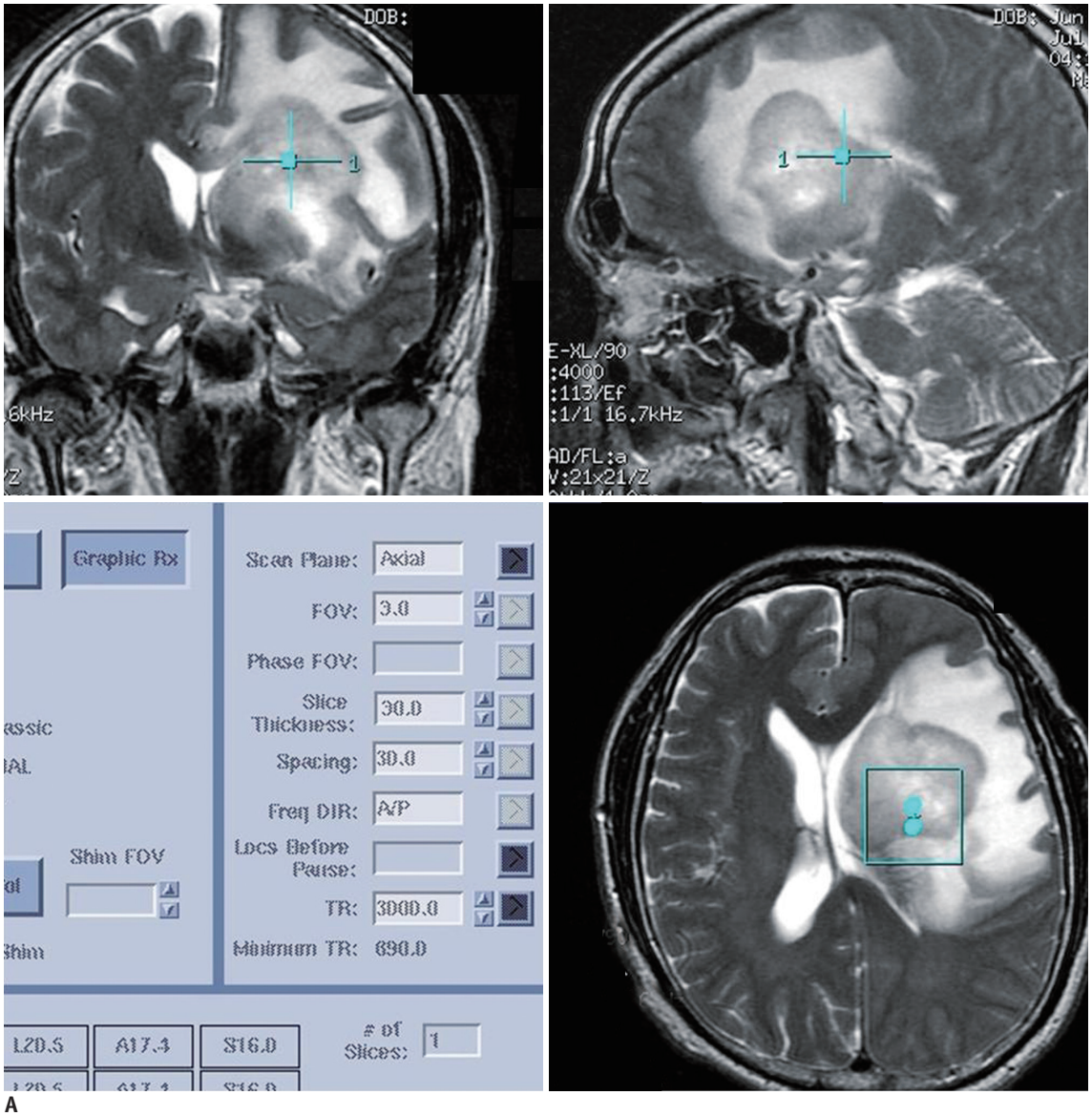

A

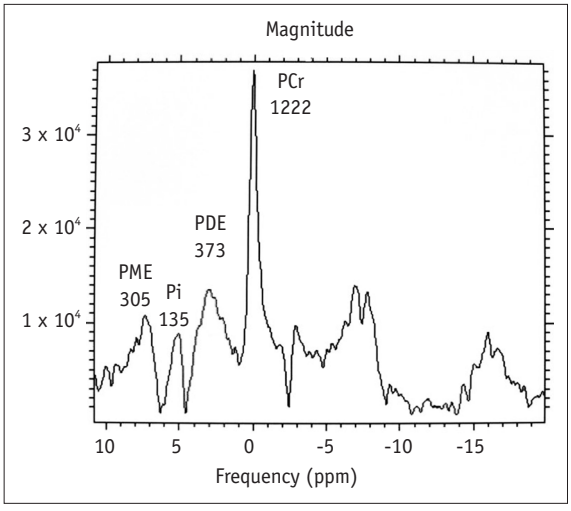

B

Fig. 4. 53-year-old man with large B cell lymphoma.
A. Localizer image for ^{31}P MRS shows large mass with marked surrounding edema in left basal ganglia area. **B.** ^{31}P MRS shows high level of PME (305), high level of PCr (1222) and low level of PDE (373). Calculated ratio shows high PME/PDE ratio (0.81). Calculated PDE/Pi ratio (2.76) is lower than its mean value of control group (3.44) and astrocytoma group (3.27). Calculated PDE/PCr ratio (0.31) is also lower than that of astrocytoma group (0.77). PME = phosphomonoester, PDE = phosphodiester, PCr = phosphocreatine, MRS = magnetic resonance spectroscopy, Pi = inorganic phosphate

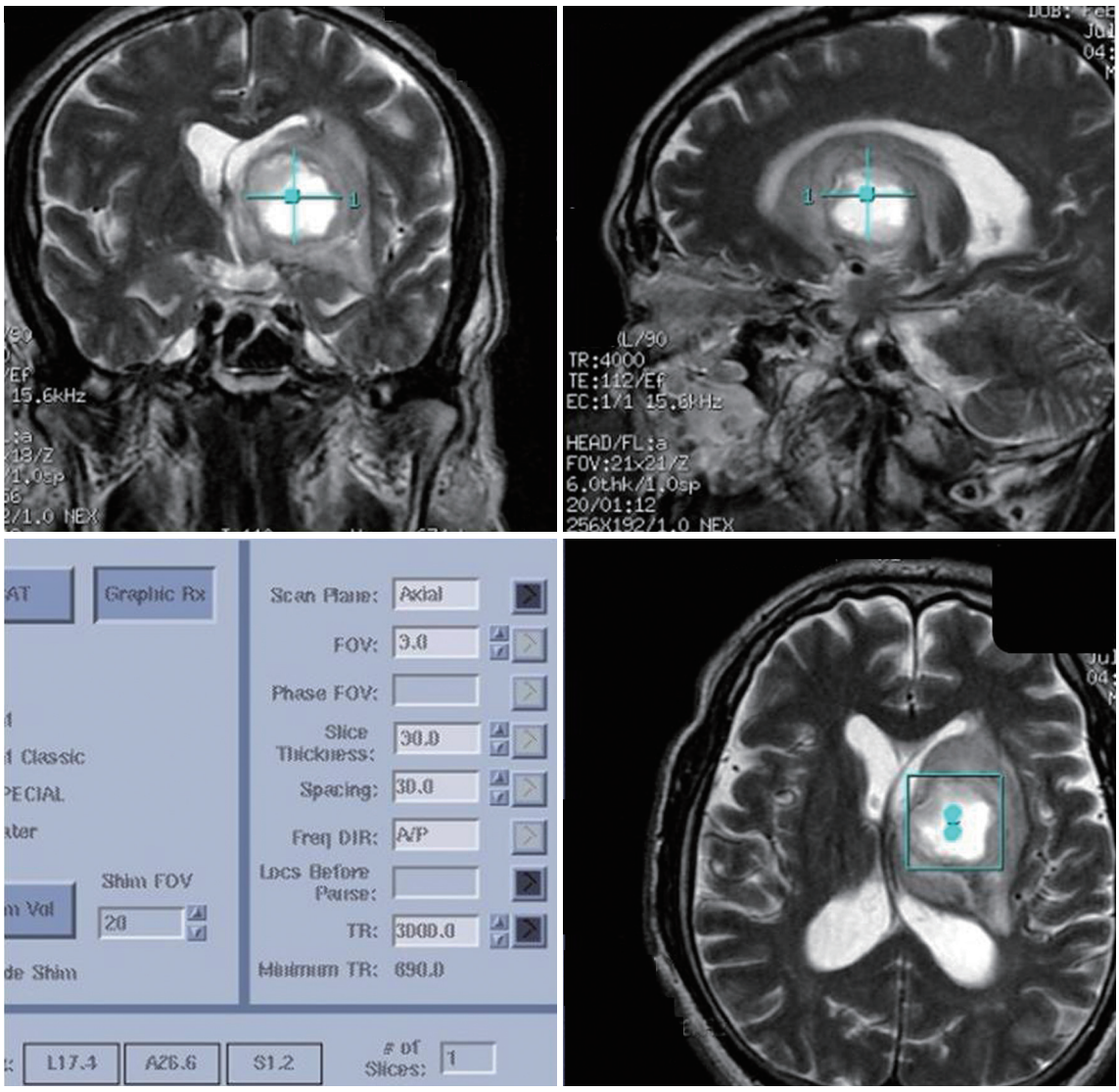

A

Fig. 5. 73-year-old man with brain abscess.
A. FID signal for ^{31}P MRS was obtained at left basal ganglia mass lesion.

metastasis showed a wide standard deviation. Two cases of metastasis showed a lower pH value (below 6.90) than that in the normal brain. Three cases of metastasis showed marked alkalization. The pH in the brain abscess (7.56 ± 0.64) also showed a wide standard deviation, compared to that in the control group (*p* value, 0.159).

The ratios of PME/PDE, PDE/Pi, PME/PCr and PDE/PCr showed statistical significant differences between each brain lesion groups by using the Kruskal-Wallis test (Table 2). We used the Dunn procedure for comparison of each group and a *p* value of less than 0.005 was considered significant. The PME/PDE ratio in the astrocyoma group (0.56 ± 0.10) was significantly higher than that in the control group (0.47 ± 0.07) (*p* value, 0.003). The PME/PDE ratio in the lymphoma group (0.60 ± 0.15) was higher than that in the control group, but it had a wide standard deviation (*p* value, 0.117). The mean value of the PME/PDE ratio in metastasis (0.68 ± 0.19) was significantly higher than that in the control group (*p* value, 0.003). The abscess group showed a higher mean value of the PME/PDE ratio (0.65 ± 0.32) with a wide standard deviation than that in control group, statistically insignificant (*p* value, 0.366).

The PDE/Pi ratio in the lymphoma group (2.57 ± 0.60) was significantly lower than that in the control group (3.44 ± 0.49) (*p* value, 0.002). The PDE/Pi ratio in lymphoma was lower than that in astrocytoma (3.27 ± 0.62), but statistically insignificant (*p* value, 0.052). The PME/PCr ratio in the astrocyoma (0.43 ± 0.11) was significantly

Korean Journal of Radiology
KJR

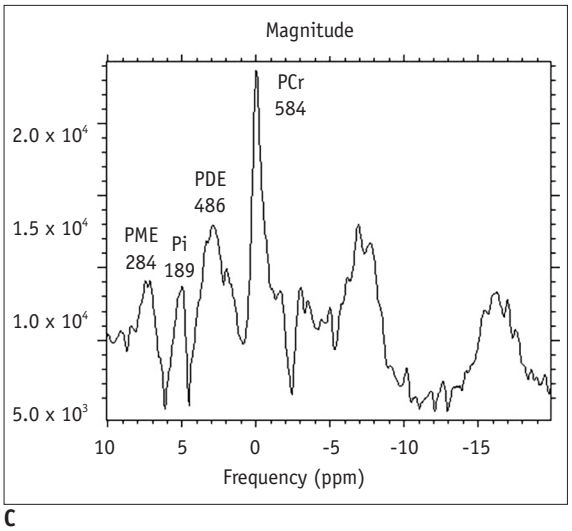

B C

Fig. 5. 73-year-old man with brain abscess.
B. Fluid-attenuated inversion recovery image shows heterogeneous signal intensity mass with central low signal intensity in left basal ganglia.
C. ^{31}P MRS shows low level of PME (284), low level of PCr (584) and relatively high level of PDE (486). Calculated ratio of PME/PDE (0.58) is lower than its mean value of metastasis group (0.68). FID = free induction decay, PME = phosphomonoester, PDE = phosphodiester, PCr = phosphocreatine, MRS = magnetic resonance spectroscopy, Pi = inorganic phosphate

Table 1. Mean pH and Mean Metabolite Ratios (± SD) between Normal Control Group and Brain Tumor Group

	Normal Control (n = 11) Mean ± SD	Brain Tumor (n = 22) Mean ± SD	*P**
pH	7.07 ± 0.10	7.28 ± 0.27	0.090
PME/PDE	0.47 ± 0.07	0.57 ± 0.11	0.012
PME/Pi	1.60 ± 0.19	1.80 ± 0.51	0.178
PDE/Pi	3.44 ± 0.49	3.16 ± 0.74	0.088
PME/ATP	0.21 ± 0.03	0.24 ± 0.05	0.261
PDE/ATP	0.45 ± 0.09	0.43 ± 0.11	0.559
PME/PCr	0.34 ± 0.07	0.40 ± 0.12	0.178
PDE/PCr	0.75 ± 0.20	0.72 ± 0.21	0.753
PCr/ATP	0.61 ± 0.07	0.61 ± 0.14	1.000
PCr/Pi	4.74 ± 0.74	4.63 ± 1.42	0.445
ATP/Pi	7.76 ± 0.64	7.93 ± 2.81	0.822

Note.— *All *p* values were calculated by using Mann-Whitney U test. SD = standard deviation, PME = phosphomonoester, PDE = phosphodiester, PCr = phosphocreatine, ATP = adenosine triphosphate, Pi = inorganic phosphate

higher than that in the control group (0.34 ± 0.07) and in the lymphoma group (0.30 ± 0.08) (*p* value, 0.004, 0.003, respectively). The PME/PCr in lymphoma was also reduced compared to that of the control group, although the difference was statistically insignificant (*p* value, 0.151). The PDE/PCr ratio in lymphoma (0.51 ± 0.16) was significantly lower than that in the astrocytoma group (0.77 ± 0.18) (*p* value, 0.002). The PDE/PCr ratio in the lymphoma group was reduced compared to that of the control group (0.75 ± 0.20), but the statistically insignificant *p* value was observed (0.068).

There was no significant parameter between the low grade astrocytoma and high grade astrocytoma (Table 3). All the parameters of the metabolite ratios did not show significant differences between the brain tumor and the abscess (Table 3).

DISCUSSION

^{31}P magnetic resonance spectroscopy can monitor the intracellular pH in living systems by using the chemical shifts of various phosphorous compounds (13). We obtained the intracellular pH by using the chemical shift of endogeneous Pi. The microenvironment within solid tumors displays acidic and hypoxic physiochemical alterations (14, 15). Contrary to the assumption that tumor cells have acidic metabolism, measurements of human and animal tumor pH using ^{31}P MRS reported neutral-to-alkaline values (16). As reported in various studies, the pH of brain tumors was significantly higher than that of the normal brain tissue (17, 18).

Table 2. Mean pH and Mean Metabolite Ratios (± SD) in Normal Control Group, Astrocytoma Group, Lymphoma Group, Metastasis Group and Abscess Group

	Normal Control (n = 11) Mean ± SD	Astrocytoma (n = 13) Mean ± SD	Lymphoma (n = 4) Mean ± SD	Metastasis (n = 5) Mean ± SD	Abscess (n = 6) Mean ± SD	*P**
pH	7.07 ± 0.10	7.15 ± 0.20	7.45 ± 0.32	7.48 ± 0.56	7.56 ± 0.64	0.058
PME/PDE	0.47 ± 0.07	0.56 ± 0.10	0.60 ± 0.15	0.68 ± 0.19	0.65 ± 0.32	0.034
PME/Pi	1.60 ± 0.19	1.83 ± 0.50	1.56 ± 0.61	1.69 ± 0.35	2.00 ± 1.01	0.304
PDE/Pi	3.44 ± 0.49	3.27 ± 0.62	2.57 ± 0.60	2.76 ± 1.27	3.18 ± 0.78	0.039
PME/ATP	0.21 ± 0.03	0.24 ± 0.05	0.20 ± 0.05	0.23 ± 0.04	0.28 ± 0.08	0.152
PDE/ATP	0.45 ± 0.09	0.44 ± 0.10	0.35 ± 0.11	0.37 ± 0.15	0.48 ± 0.18	0.340
PME/PCr	0.34 ± 0.07	0.43 ± 0.11	0.30 ± 0.08	0.36 ± 0.10	0.42 ± 0.09	0.028
PDE/PCr	0.75 ± 0.20	0.77 ± 0.18	0.51 ± 0.16	0.59 ± 0.28	0.73 ± 0.27	0.049
PCr/ATP	0.61 ± 0.07	0.58 ± 0.15	0.69 ± 0.12	0.66 ± 0.11	0.67 ± 0.13	0.314
PCr/Pi	4.74 ± 0.74	4.36 ± 0.95	5.51 ± 2.52	4.72 ± 0.48	4.86 ± 2.18	0.640
ATP/Pi	7.76 ± 0.64	7.90 ± 2.51	8.37 ± 4.34	7.28 ± 1.39	7.61 ± 4.12	1.000

Note.— *All *p* values were calculated by using Kruskal-Wallis test. SD = standard deviation, PME = phosphomonoester, PDE = phosphodiester, PCr = phosphocreatine, ATP = adenosine triphosphate, Pi = inorganic phosphate

Table 3. Significant Differences of pH and Metabolite Ratios between Low Grade Astrocytoma Group and High Grade Astrocytoma Group and between Brain Tumor Group and Abscess Group

	Low Grade vs. High Grade Astrocytoma *P**	Brain Tumor vs. Abscess *P**
pH	0.575	0.419
PME/PDE	0.877	0.947
PME/Pi	0.758	0.689
PDE/Pi	0.165	0.505
PME/ATP	0.280	0.182
PDE/ATP	0.440	0.386
PME/PCr	1.000	0.594
PDE/PCr	0.758	0.947
PCr/ATP	0.877	0.317
PCr/Pi	0.537	0.594
ATP/Pi	0.758	0.463

Note.— *All *p* values were calculated by using Mann-Whitney U test. PME = phosphomonoester, PDE = phosphodiester, PCr = phosphocreatine, ATP = adenosine triphosphate, Pi = inorganic phosphate

In our study, the brain tumor had a tendency of alkalization. The pH of astrocytoma was slightly higher than that of the normal brain. In lymphoma, the pH was significantly higher than that in the normal brain. The pH in the abscesses and metastatic lesions was clearly higher than that in the normal brain, but the pH was not statistically different due to the large scatter of data. We suspected that this was caused by the heterogenous nature of the lesions.

The phosphorous metabolites, detected by ^{31}P MRS, can be used for providing the information of the phospholipid metabolism. The measuring of the absolute concentration of phosphorous metabolites is the ultimate goal of the ^{31}P MRS study. However, there are various limitations. The obtained integral of each phosphorous metabolites (PME, PDE, PCr, Pi, ATP) on the spectrum were considered as the relative concentration of metabolites in the lesion (4). The difficulty of appropriate calibration, the sensitivity of the surface coils, J-coupling, low concentration of metabolites and variations from other various correction factors also contribute to the variations of quantification of phosphorus metabolites. The use of metabolite ratios could reduce these variations. A number of researchers have used various ratios of metabolic components, such as PME/ATP, PDE/ATP, PDE/PME, PCr/ATP, PME/PCr PDE/PCr and etc (3, 8, 19).

The PME and PDE indicated the significance of phospholipid precursors and catabolites as markers for tumor detection, malignancy, progression and the response to treatment (3, 5, 20). The major components of PME are phosphocholine (PCho) and phosphoethanolamine (PEtn) (19). These molecules are the intermediates in the biosynthesis of phosphoglycerides and indicate the presence of precursors of cytoplasmic membrane synthesis (21). The complete deacylation of phospholipids produce glycerophosphocholine and glycerophosphoethanolamine. These molecules are the major components of PDE, which indicates the presence of breakdown products of the membrane (21, 22). The ratio of PME/PDE can serve as an index of the metabolism of membrane phospholipid

Korean Journal of Radiology
KJR

and reflect changes in the rate of membrane synthesis or metabolic turnover (5, 8).

We observed significantly increased PME/PDE ratio in brain tumor as compared to that in the normal brain control group. We also observed a significantly increased PME/PDE ratio in astrocytoma as compared to that in the normal brain. In metastasis, the PME/PDE ratio was significantly higher than that in the normal brain. The PME/PDE ratio in lymphoma was higher than that in the normal brain and astrocytoma, but this was statistically insignificant.

Unfortunately, these changes have variable limitations in application to the tumors, according to the previous studies. At first, both PME level and PDE level was increased in most tumors (8). It seems difficult to understand an accumulation of metabolic precursors with an accelerated formation of end products. Various pathways, enzymes and the roles of PCho and PEtn can affect this paradoxical phenomenon. Furthermore, other studies also showed increased PME levels with using cytostatic agents on the cancer cells, which inhibit proliferation (20, 23). Moreover, these alterations are not exclusive to malignancy (8). These changes may also occur in developing (embryo or fetal) organs, in proliferating tissues, such as regenerating liver, in benign tumors and even in some degenerative pathologies (8).

Variability of peak intensities of the phosphorous metabolite on ^{31}P MRS was also demonstrated, according to the different origin of the tumors (24). In the present study, the PME/PCr and PDE/PCr ratios in lymphoma were also significantly lower than those in the astrocytoma group.

The PDE/Pi ratio in the lymphoma group was lower than that in control group and the astrocytoma group. The ratio of PDE/PCr in lymphoma was significantly lower than that in astrocytoma. We suspected that this observation may be correlated with the reduced PDE level in lymphoma. The PME/PCr and PDE/PCr ratio in lymphoma were also significantly lower than those in the astrocytoma group. On comparison with the normal control group, the PME/PCr and PDE/PCr ratios were also reduced, even thought it was statistically insignificant. We considered that this result could be correlated with the increased PCr level in lymphoma. We thought that these changes will be helpful to differentiate the brain tumors.

There are reports of phosphorous metabolites as markers for the degree of malignancy (3, 6). In this study, there was no statistically significant parameter that would differentiate between low grade astrocytoma and high grade astrocytoma.

Another biologic application of ^{31}P MRS is studying the cellular energy metabolism. ATP, PCr and Pi play crucial roles in cellular energetic (25-27). In a study on brain tumor, the Pi/PCr ratio was significantly elevated and the PCr/ATP ratio was reduced (19). The PCr/ATP, PCr/Pi and ATP/Pi ratios in this study were not significantly different between the control group and the brain tumor group, and between each brain lesion.

In the present study, the MRS signal was obtained by using the FID 2D CSI sequence, collecting FID signal using the CSI sequence. In a classical CSI sequences, the MRS obtains the signal by applying the phase-encoding gradients without a frequency-encoding gradient. Thus, the FID CSI sequence collects a FID, either from the entire sensitive volume of the receiver coil or a prescribed set of slices (28, 29). As a result, the MRS signals using the FID CSI sequences can be contaminated from normal parenchyma in the outside of the lesion. The MRS signal differences between the tumor and normal tissue can be reduced. For more conservative approach, we performed ^{31}P MRS on the relatively large sized brain tumor.

^{31}P magnetic resonance spectroscopy study to the patients with a low field strength equipment like a 1.5 T scanner usually require a long scan time and large voxel, due to low SNR caused by a low concentration of phosphorous metabolite in the lesion (3, 8). Recently, MRS apparatus has rapidly evolved to perform the study of a relatively small volume of voxel and in a reasonable scan time. We adapted a 27 mL voxel volume and a 6 minutes 36 seconds scan time, with a total scan time of 15 minutes, including the scanning for localization. We designed this study to obtain the MRS signal *in vivo* as soon as possible and to evaluate the clinical feasibility of ^{31}P MRS study. This scan time was tolerable for patients to obtain the MR imaging and the MR spectrum in a study.

^{31}P magnetic resonance spectroscopy study of human brain lesions has shown substantial variability. This variability reported in the literature seemed to have numerous causes. In another previous study (3), masses with a large portion of necrosis were excluded. They suspected that the amount of the necrosis or cystic portion in the brain tumor could create variability of the peak intensities of phosphorous metabolites in the same tumor group. Moreover, the peripheral located voxel and hemorrhage in a lesion may produce magnetic susceptibility artifact that causes a non-diagnostic spectrum or distortion of spectrum. In order to

avoid the possibility of spectrum diversity by these causes, we excluded the brain lesions that have a large cyst, a large necrotic portion, hemorrhage, and were small peripheral located brain lesions, according to the routine brain MRI.

Conclusion

The clinically applicable ^{31}P MRS spectrum was obtained with a relatively short scan time and the pH, PME/PDE, PDE/Pi, PME/PCr, and PDE/PCr ratios seem to be useful parameters for the differentiation of the brain tumors.

REFERENCES

1. Stubbs M, Rodrigues LM, Gusterson BA, Griffiths JR. Monitoring tumor growth and regression by 31P magnetic resonance spectroscopy. *Adv Enzyme Regul* 1990;30:217-230
2. Podo F, Canevari S, Canese R, Pisanu ME, Ricci A, Iorio E. MR evaluation of response to targeted treatment in cancer cells. *NMR Biomed* 2011;24:648-672
3. Park JM, Park JH. Human in-vivo 31P MR spectroscopy of benign and malignant breast tumors. *Korean J Radiol* 2001;2:80-86
4. Cohen JS. Phospholipid and energy metabolism of cancer cells monitored by 31P magnetic resonance spectroscopy: possible clinical significance. *Mayo Clin Proc* 1988;63:1199-1207
5. Lehnhardt FG, Röhn G, Ernestus RI, Grüne M, Hoehn M. 1H- and (31)P-MR spectroscopy of primary and recurrent human brain tumors in vitro: malignancy-characteristic profiles of water soluble and lipophilic spectral components. *NMR Biomed* 2001;14:307-317
6. Heiss WD, Heindel W, Herholz K, Rudolf J, Bunke J, Jeske J, et al. Positron emission tomography of fluorine-18-deoxyglucose and image-guided phosphorus-31 magnetic resonance spectroscopy in brain tumors. *J Nucl Med* 1990;31:302-310
7. Hirakawa K, Naruse S, Higuchi T, Horikawa Y, Tanaka C, Ebisu T. The investigation of experimental brain tumours using 31P-MRS and 1H-MRI. *Acta Neurochir Suppl (Wien)* 1988;43:140-144
8. Maintz D, Heindel W, Kugel H, Jaeger R, Lackner KJ. Phosphorus-31 MR spectroscopy of normal adult human brain and brain tumours. *NMR Biomed* 2002;15:18-27
9. Arias-Mendoza F, Payne GS, Zakian KL, Schwarz AJ, Stubbs M, Stoyanova R, et al. In vivo 31P MR spectral patterns and reproducibility in cancer patients studied in a multi-institutional trial. *NMR Biomed* 2006;19:504-512
10. Ng TC, Majors AW, Vijayakumar S, Baldwin NJ, Thomas FJ, Koumoundouros I, et al. Human neoplasm pH and response to radiation therapy: P-31 MR spectroscopy studies in situ. *Radiology* 1989;170(3 Pt 1):875-878
11. Estève F, Grand S, Rubin C, Hoffmann D, Pasquier B, Graveron-Demilly D, et al. MR spectroscopy of bilateral thalamic gliomas. *AJNR Am J Neuroradiol* 1999;20:876-881
12. Oberhaensli RD, Galloway GJ, Hilton-Jones D, Bore PJ, Styles P, Rajagopalan B, et al. The study of human organs by phosphorus-31 topical magnetic resonance spectroscopy. *Br J Radiol* 1987;60:367-373
13. Madden A, Leach MO, Sharp JC, Collins DJ, Easton D. A quantitative analysis of the accuracy of in vivo pH measurements with 31P NMR spectroscopy: assessment of pH measurement methodology. *NMR Biomed* 1991;4:1-11
14. Gillies RJ, Raghunand N, Karczmar GS, Bhujwalla ZM. MRI of the tumor microenvironment. *J Magn Reson Imaging* 2002;16:430-450
15. Griffiths JR. Are cancer cells acidic? *Br J Cancer* 1991;64:425-427
16. Negendank W. Studies of human tumors by MRS: a review. *NMR Biomed* 1992;5:303-324
17. Hubesch B, Sappey-Marinier D, Roth K, Meyerhoff DJ, Matson GB, Weiner MW. P-31 MR spectroscopy of normal human brain and brain tumors. *Radiology* 1990;174:401-409
18. Okada Y, Kloiber O, Hossmann KA. Regional metabolism in experimental brain tumors in cats: relationship with acid/base, water, and electrolyte homeostasis. *J Neurosurg* 1992;77:917-926
19. Albers MJ, Krieger MD, Gonzalez-Gomez I, Gilles FH, McComb JG, Nelson MD Jr, et al. Proton-decoupled 31P MRS in untreated pediatric brain tumors. *Magn Reson Med* 2005;53:22-29
20. Neeman M, Degani H. Metabolic studies of estrogen- and tamoxifen-treated human breast cancer cells by nuclear magnetic resonance spectroscopy. *Cancer Res* 1989;49:589-594
21. Aisen AM, Chenevert TL. MR spectroscopy: clinical perspective. *Radiology* 1989;173:593-599
22. Podo F. Tumour phospholipid metabolism. *NMR Biomed* 1999;12:413-439
23. Abraha A, Shim H, Wehrle JP, Glickson JD. Inhibition of tumor cell proliferation by dexamethasone: 31P NMR studies of RIF-1 fibrosarcoma cells perfused in vitro. *NMR Biomed* 1996;9:173-178
24. Arnold DL, Emrich JF, Shoubridge EA, Villemure JG, Feindel W. Characterization of astrocytomas, meningiomas, and pituitary adenomas by phosphorus magnetic resonance spectroscopy. *J Neurosurg* 1991;74:447-453
25. Kemp GJ, Meyerspeer M, Moser E. Absolute quantification of phosphorus metabolite concentrations in human muscle in vivo by 31P MRS: a quantitative review. *NMR Biomed* 2007;20:555-565
26. Burkhard T, Herzog C, Linzbach S, Spyridopoulos I, Huebner F, Vogl TJ. Cardiac (31)P-MRS compared to echocardiographic findings in patients with hypertensive heart disease without overt systolic dysfunction--preliminary results. *Eur J Radiol* 2009;71:69-74
27. Schulz UG, Blamire AM, Davies P, Styles P, Rothwell PM. Normal cortical energy metabolism in migrainous stroke: A 31P-MR spectroscopy study. *Stroke* 2009;40:3740-3744
28. Skoch A, Jiru F, Bunke J. Spectroscopic imaging: basic principles. *Eur J Radiol* 2008;67:230-239
29. Keevil SF, Newbold MC. The performance of volume selection sequences for in vivo NMR spectroscopy: implications for quantitative MRS. *Magn Reson Imaging* 2001;19:1217-1226